学術論文

TiO_2-VO_2二成分系スピノーダル分解におけるマイクロ波照射効果

Microwave irradiation effects on the spinodal decomposition of TiO_2-VO_2 system

青柳 宗一郎、福島 潤*、林 大和、滝澤 博胤

東北大学大学院 工学研究科
〒980-8579　宮城県仙台市青葉区荒巻字青葉 6-6-07

Department of Applied Chemistry, School of Engineering, Tohoku University
6-6-07, Aoba, Aramaki, Aoba-ku, Sendai, 980-8579, Japan

corresponding author*, e-mail address: fukushima@aim.che.tohoku.ac.jp
Keywords: microwave heating, spinodal decomposition, selective heating, metal−insulator transition, VO_2, TiO_2

Abstract

In this study, TiO_2–VO_2 solid solutions were heated by microwaves and by an electric-furnace to investigate the spinodal decomposition behavior of a TiO_2–VO_2 system. Single-mode and multi-mode type microwave irradiation devices were used to investigate the spinodal decomposition of TiO_2–VO_2. In the conventional process, spinodal decomposition required 12 h of annealing. However, in the microwave process, spinodal decomposition proceeded at a low temperature for 30 min. Additionally, the metal–insulator transition temperature (T_{MI}) of the prepared sample was lower than that of pristine VO_2. This indicated the existence of anisotropic pressure on the boundary between the Ti-rich phase and the V-rich phase. Furthermore, the microwave-irradiated samples exhibited broadened double endothermic peaks in the DSC profiles. The broad peaks indicated that the samples exhibit several values of T_{MI}, implying variations in the composition of the V-rich phase. The phase variation resulted from the selective heating of the V-rich layer that induced one-directional material diffusion from the V-rich phase to the Ti-rich phase.

1. Introduction

The metal−insulator transition temperature (T_{MI}) of vanadium dioxides (VO_2) is approximately 69 °C. Hence, VO_2 behaves like a metal at temperatures exceeding 69 °C and an insulator at temperatures below the same. Metal−insulator transition is due to the transformation of the crystal structure from tetragonal (P42/mnm) rutile (R) in the high-temperature region to monoclinic (P21/c) at T_{MI} at a low temperature[1]. The time taken for complete phase transition is on the sub picosecond scale[2], and there are significant changes in the optical absorption and resistivity across the transition[3]. Therefore, VO_2 may be applied to ultrafast optical switching devices and thermochromic materials[4-8].

Applications involving thermochromic materials require effective control of T_{MI}. Previous studies indicate that the T_{MI} value of VO_2 increases with isotropic pressure (0.6 K/GPa)

and decreases with anisotropic pressure along the *c*-axis (-12 K/GPa)[9]. Another study reported that T_{MI} alternatively decreases along the *c*-axis through the spinodal decomposition of TiO_2-VO_2 system. In the spinodal decomposition, an epitaxial layer is selectively formed along the *c*-axis because the difference in their *c*-axis lattice parameters exceeds that along the *a*-axis [10]. Another method to decrease T_{MI} involves stacking a VO_2 nanolayer on a substrate to induce anisotropic pressure between VO_2 and the substrate. The VO_2 thin film is prepared by various methods, including pulse laser decomposition (PLD), physical vapor decomposition (PVD), and magnetron spattering[11-15]. Among these, spinodal decomposition is the simplest and easiest method to decrease T_{MI} since solid state reactions, which involve mixing powders, pressing them into pellets, and heating in a furnace, are employed.

Intrinsically, solid-state reactions involve prolong high-temperature treatment. Hence, they are time- and energy-consuming processes. Specifically, the spinodal decomposition of VO_2 and TiO_2 requires several hours[10]. In order to shorten the time and decrease the process temperature, the present study focuses on microwave processing. A previous study used microwave processing and reported a decrease in solid-state reaction time. For example, the study reported on the increase in material transfer between $SrTiO_3$ and $CaTiO_3$[16] and rapid synthesis of $Fe_2O_3(ZnO)_m$[17]. Another report demonstrated that the spinodal decomposition of a TiO_2–SnO_2 system was accelerated with microwave irradiation[18]. Furthermore, the authors suggested that only SnO_2 was associated with high temperature in a TiO_2–SnO_2 system and that these anisothermal conditions led to spinodal decomposition within a short period. In addition to the TiO_2–SnO_2 system, it is considered that the anisothermal conditions occurred in the TiO_2–VO_2 system because VO_2 was selectively heated.

In the present study, a solid solution of TiO_2–VO_2 was subjected to microwave irradiation to investigate the spinodal decomposition behavior of the TiO_2–VO_2 system. The composition and phase transition temperature of the microwave-irradiated system were compared with those of the conventionally processed system.

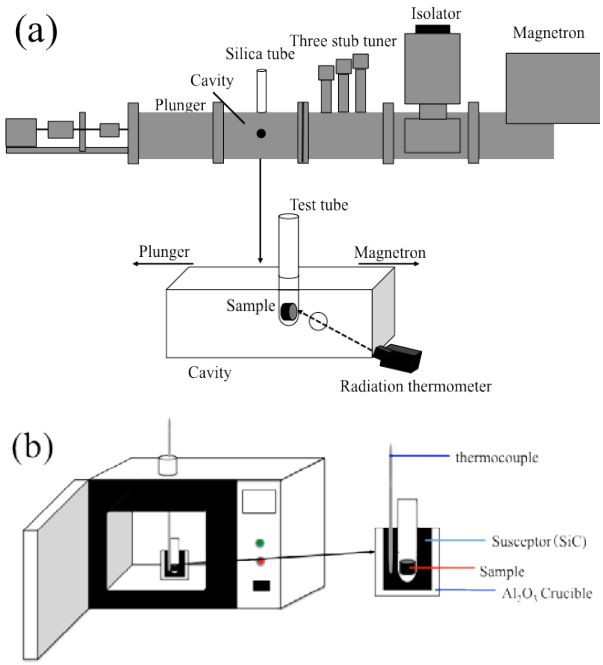

Fig. 1: Schematic view of the microwave irradiation device of single-mode type (a), multi-mode type (b).

2. Experimental procedure

Two types of microwave irradiation devices were used to investigate the spinodal decomposition of TiO_2–VO_2. Figure 1 shows the schematic views of each of the devices. One of the devices was a single-mode type microwave irradiation device. The device was composed of a magnetron (IMP-15ENA IDX Co., Ltd., Tochigi, Japan), an isolator, three stub tuners, a plunger, and a TE102 cavity, which specially divided the maximum point of E-field and H-field intensity. The sample was inserted into a test tube composed of quartz and sealed in a vacuum. The sample temperature was measured by a radiation thermometer through a hole at the side of the cavity. The other device was a multi-mode type microwave irradiation device, μReactor Ex (Shikoku Keisoku Co., Ltd., Takamatsu, Japan), as shown in Fig. 1 (b). In this device, microwaves were uniformly irradiated to a sample. The sample was also sealed in a test tube, and the test tube was surrounded by SiC, which acted as a susceptor. We measured the susceptor temperature, as it is close to the

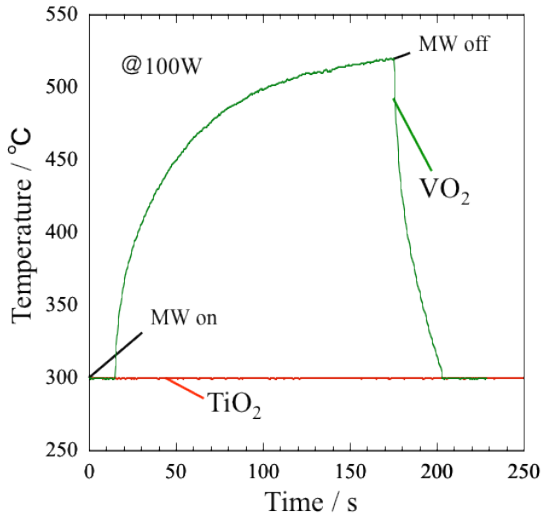

Fig. 2: Microwave absorption properties of TiO_2 and VO_2

sample temperature given the susceptor absorbs most of the microwave energy.

The solid solution $Ti_{0.4}V_{0.6}O_2$ was prepared from a mixture of TiO_2 (99.9%, 2 μm, Kojundo Chemical Laboratory Co., Ltd., Saitama, Japan), V_2O_5 (99.0% Wako Pure Chemical Industries, Ltd. Osaka, Japan), and V_2O_3 (99.9%, 180 μm, Kojundo Chemical Laboratory Co., Ltd., Saitama, Japan). The powders were mixed with ethanol with an agate mortar and a pestle and dried. The dried powder was pressed into a pellet (diameter: ⌀ 6 mm, height: 2.5 mm) and sealed into a quartz test tube. The sample was heated at 600 °C for 1 d, and a solid solution was obtained by rapid quenching. The solid solution pellet was sealed into quartz test tube, and heated by each of the microwave irradiation devices for 30 min at 300, 400 and 500 °C. For comparison with microwave processing, a conventionally heated sample was prepared by using an electric furnace at 900 °C for 1 h and then heated at 400 °C for 12 h.

All products were examined by powder X-ray diffraction (XRD RINT-2000PC Rigaku Co., Tokyo, Japan) using Cu-Kα radiation to determine the lattice parameters. The microstructure of the sample was observed by using scanning transmission electron microscopy (STEM, HD-2700 Hitachi High-Technologies Co., Tokyo, Japan) and an energy-dispersive X-ray (EDX) analyzer. Differential scanning calorimetry (DSC Q2000, TA Instruments Japan Inc., Tokyo, Japan)) was used to determine T_{MI}.

3. Results and discussion

3-1. Spinodal decomposition by microwave irradiation

In this system, the microwave energy absorbed by VO_2 exceeds that absorbed by TiO_2. Figure 2 shows the microwave absorption properties of TiO_2 and VO_2. In order to investigate the microwave absorption properties, each material was subjected to microwave irradiation from a single-mode cavity and the temperature was measured. Each powder was pelletized and set in the quartz test tube, and the

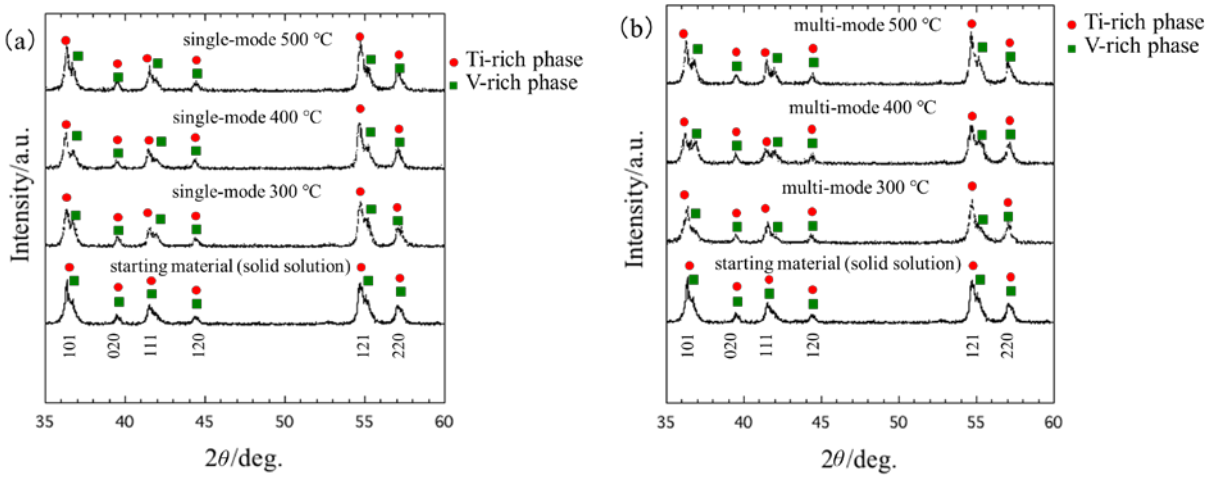

Fig. 3: XRD patterns of samples prepared by the single-mode microwave furnace (a) and multi-mode furnace (b).

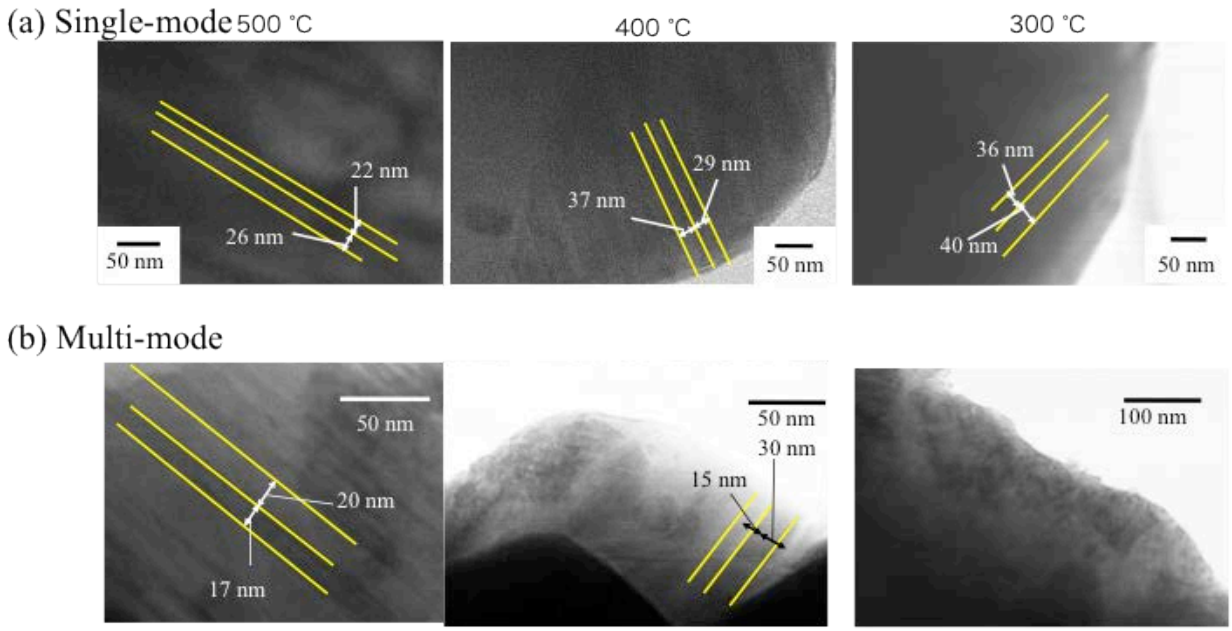

Fig. 4: STEM images of the sample prepared approximately at 300, 400 and 500 °C by (a) the single-mode microwave furnace and (b) the multi-mode microwave furnace.

test tube was set at the point of H-field intensity maxima. The temperature of TiO_2 did not increase, although that of VO_2 immediately increased after commencing the microwave irradiation. The resistivity of TiO_2 is 10^7 Ω cm although that of VO_2 is 10^{-2} Ω cm. During H-field heating, conductive materials are likely to absorb microwave energy. Thus, VO_2 is selectively heated in the system during microwave irradiation.

Figures 3(a) and (b) show the XRD patterns of the samples prepared by using the single-mode and multi-mode microwave irradiation devices, respectively. All the irradiated samples exhibited peaks with *hk*0 reflections that were the same as those of a starting solid-solution sample: the (020) and (220) peaks were not split, and this implied that *a*-axis lengths between the two phases are equal. However, peaks with $l \neq 0$, such as (101), (111), and (121), were split into two sets of peaks, thereby indicating differences in *c*-axis length of two phases. The $l \neq 0$ peaks of the decomposed samples at low and high 2θ values corresponded to the Ti-rich and V-rich phases, respectively. The *a*-axis length of TiO_2 exceeded that of VO_2 to maintain the cell volume, and thus, a misfit strain between these two phases forced the *c*-axis length to increase and decrease in the Ti-rich and V-rich phases, respectively. The width of the split peaks increased with a decrease in the holding temperature. This suggests that the difference in lattice parameters along the *c*-axis increased between the Ti-rich and V-rich phases. The results corresponded to the phase diagram obtained in a previous study[10]. Peaks of $l \neq 0$ at 300 °C in the multi-mode did not clearly show the split. However, peaks of $l \neq 0$ at 400 °C and 500 °C were split, and the lattice parameter along the *c*-axis between the Ti-rich and V-rich phase increased when the holding temperature was low. The absence of spinodal decomposition at 300 °C in multi-mode irradiation could be attributed to susceptor heating. Although the susceptor contributed to the stabilization of the holding temperature, it prevented spinodal decomposition in a short period because the thermal effect was dominant.

Figure 4 (a) shows STEM images of the sample prepared by the single-mode microwave furnace at 300, 400 and 500 °C for 30 min, and Figure 4 (b) shows STEM images of the sample prepared by the multi-mode microwave furnace in the same conditions. With the exception of the sample prepared at 300 °C by the multi-mode microwave furnace, STEM images of all samples showed a layer (with a few

Table1: Volume of unit cell and Ti content calculated from lattice parameters obtained from the XRD results

	Ti-rich phase		V-rich phase	
	unit cell V (10^{-3} nm^3)	Ti content	unit cell V (10^{-3} nm^3)	Ti content
Multi-mode	61.36	0.573	59.81	0.166
Single-mode	61.23	0.534	59.99	0.208
conventional heating 900 ℃→400 ℃	61.30	0.555	59.76	0.155

nanometer thickness) of bright and dark contrast stacked in a single direction. It is considered that the stacking direction is along the *c*-axis of each phase given the XRD peaks split in $l \neq 0$. The thickness of each layer was approximately 15–40 nm, and this corresponds to that in a previous study [10, 15]. The absence of a stacking structure was shown in the sample prepared at 300 °C by the multi-mode microwave furnace. This result indicated that spinodal decomposition did not proceed, and this was in agreement with the XRD results.

3-2. Behavior of spinodal decomposition in the microwave irradiation method

In order to verify the effect of microwave irradiation on the spinodal decomposition behavior, the samples prepared by microwave heating were compared with those prepared by conventional heating. Figure 5 shows the XRD patterns of each sample prepared at 400 °C for 30 min by using a multi-mode type microwave furnace, a single-mode microwave furnace, and an electric furnace and that of the sample prepared at 400 °C for 12 h after heating in an electric furnace at 900 °C for 1 h. The conditions for the sample prepared at 400 °C for 12 h after heating at 900 °C for 1 h by using electric furnace were similar to those for the sample prepared in a previous study. Thus, in this sample, the spinodal decomposition proceeded to completion and peaks with $l \neq 0$ were split. Typical split peaks with $l \neq 0$ were also detected for the microwave-irradiated samples. However, the sample prepared via the electric furnace at 400 °C for 30 min did not exhibit the fore-mentioned clear split peaks. These results suggest that spinodal decomposition preceded microwave irradiation in a short time period when compared to conventional heating.

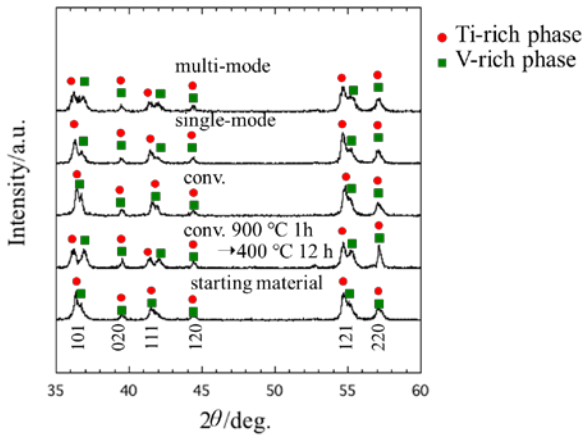

Fig. 5: XRD patterns of samples prepared by using each method

Table 1 shows that the volume of unit cell and Ti content calculated from lattice parameters obtained from the XRD results and Vegard's law[10]. The Ti content of the sample prepared by the multi-mode furnace was similar to that for the sample prepared by the electric furnace at 400 °C for 12 h after heating at 900 °C for 1 h. In contrast, the Ti content of the sample prepared by single-mode exceeded that of the sample prepared via multi-mode furnace. It is considered that the thermal effect for spinodal decomposition was dominant due to the susceptor used in the multi-mode furnace. Thus, the composition of each phase after spinodal decomposition varied with the method of heating.

Figure 6 shows the STEM images and line analyses of

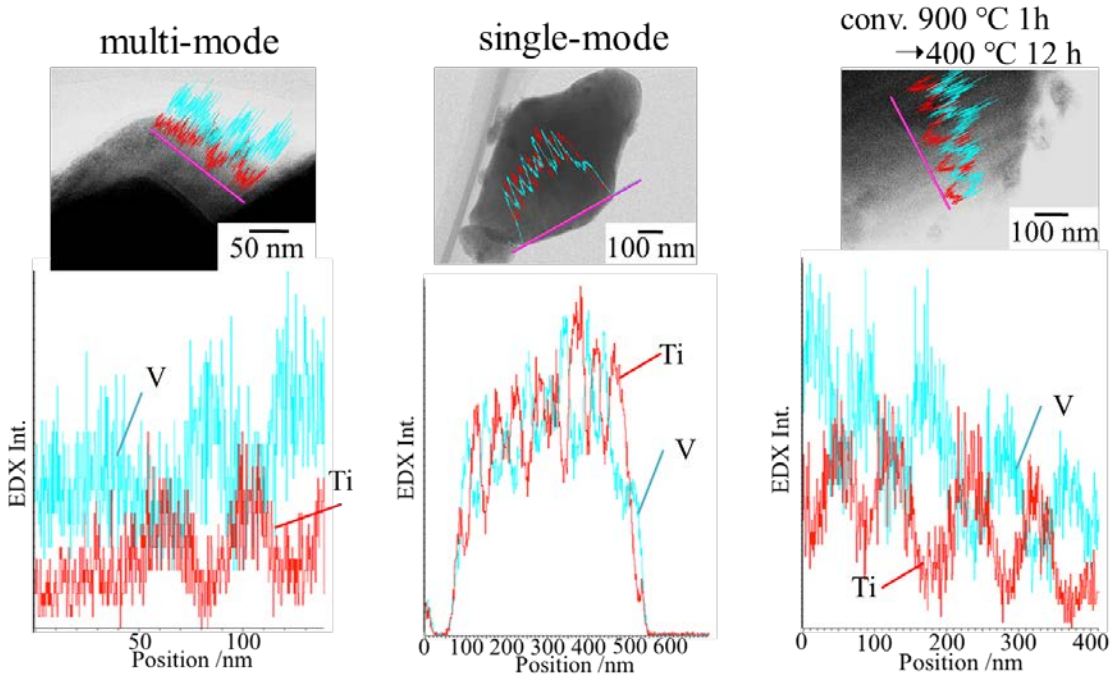

Fig. 6: STEM images and line analysis of EDX in each sample along the vertical direction of stacking layers

EDX in each sample along the vertical direction of stacking layers. The STEM images and EDX results indicate that layers of bright and dark contrast correspond to the Ti-rich phase and V-rich phase, respectively. Both samples prepared by microwave processing and conventional processing exhibited similar microstructures that consist of nanoscale-modulated layers.

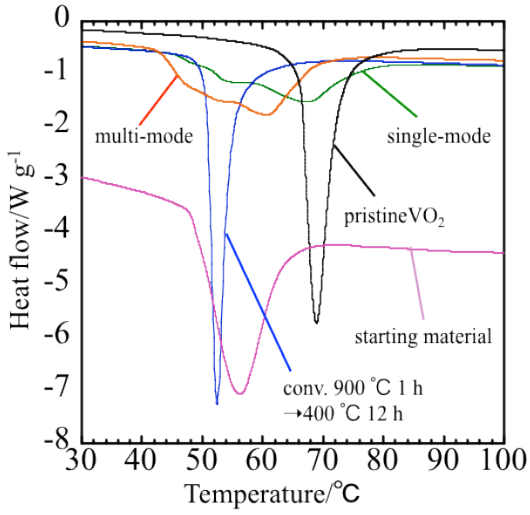

Fig. 7: DSC results of each sample

Figure 7 shows the DSC results of each sample. Latent heat requires the occurrence of the metal–insulator transition of VO_2, and this implies that T_{MI} is associated with the endothermic peak of the DSC curve. Thus, T_{MI} is determined from each endothermic peaks (Table 2). The T_{MI} of each sample decreased when compared to that of the pristine VO_2. Previous studies reported that the anisotropic pressure to VO_2 relative to the *c*-axis results in a decrease in T_{MI} by -12 K/GPa[9], and the decrease in T_{MI} indicates the existence of anisotropic pressure on the boundary between the Ti-rich phase and V-rich phase.

The microwave-irradiated samples exhibited two

Table 2: T_{MI} of each sample, as determined from DSC results

	T_{MI}(°C)
Multi-mode	42.2～42.5, 44.4～47.8
Single-mode	46.8～47.6, 49.4～50.6
conventional heating	49.9～50.7
pristine VO_2	67.0～68.0

broadened endothermic peaks. Therefore, microwave-irradiated samples exhibited several T_{MI}. The two peaks corresponded to metal–insulator transition derived from a starting solid solution and a phase formed by the microwave irradiation. Moreover, broad endothermic peaks indicated variation in the composition of the V-rich phase. This is consistent with the XRD results as the XRD peaks were also broad. In the sample prepared by the single-mode furnace, an endothermic peak was approximately close to the peak of the completely spinodal-decomposed sample, and another peak was observed on the low-temperature side of the pristine VO_2 peak. Conversely, in the sample prepared by multi-mode microwave furnace, an endothermic peak was observed at the low-temperature side of the completely spinodal-decomposed sample's peak, and another peak was observed approximately near the peak of the starting sample. We discuss the effect of microwave irradiation on the behavior of spinodal decomposition and material diffusion. In the conventional process of spinodal decomposition, a sample temperature increases above the miscibility gap curve in the first step of heating (900 °C), and then the sample is annealed at a low temperature (400 °C) to ensure concentration miscibility. Finally, a nanoscale stacked structure is achieved by autonomously developing the miscibility. In contrast, sample temperature is not uniform during microwave irradiation due to the nonuniformity of microwave electromagnetic field distribution. This temperature gradient ensures the development of concentration miscibility, and the nanoscale stacked structure is formed in a short period. Additionally, it is considered that selective heating between Ti-rich layer and V-rich layer occurs after spinodal decomposition. The selective heating induces one-directional material diffusion from the V-rich phase to Ti-rich phase and especially during single-mode microwave irradiation. One-directional material diffusion leads to various compositions of the V-rich phase when compared to those of conventional heating samples.

4. Conclusion

This study investigated the behavior of spinodal decomposition in a TiO_2–VO_2 system during microwave processing. Specifically, the TiO_2–VO_2 solid solution was used as the starting material, and spinodal decomposition proceeded within a short period (30 min). It is suggested that the development of concentration miscibility results from the nonuniform sample temperature due to the nonuniformity of the microwave electromagnetic field distribution. Additionally, the XRD and DSC results indicate that microwave selective heating induces one-directional material diffusion from the V-rich phase to Ti-rich phase, and this results in variations in the composition of the V-rich phase.

5. Acknowledgement

This study was supported by a JSPS Grant-in-Aid for Scientific Research (S) Number JP17H06156.

References

1) F. Morin, *Phys. Rev. Lett.*, **3**, (1959) 34.

2) M. Becker, A. Buckman, R. Walser et al., *Appl. Phys. Lett.*, **65**, (1994) 1507-1509.

3) M. Gurvitch, S. Luryi, A. Polyakov et al., *J. Appl. Phys.*, **102,** (2007) 033504.

4) W. Roach, I. Balberg, *Solid State Commun.*, **9,** (1971) 551-555.

5) H. Choi, J. Ahn, J. Jung et al., *Phys.l Rev. B*, **54**, (1996) 4621-4628.

6) A. Cavalleri, C. Tóth, C. Siders, et al., *Phys. Rev. Lett.*, **87**, (2001) 237401.

7) J. Yu, S. Nam, J. Lee et al., *Materials*, **9**, (2016) 556.

8) S. Kumar, F. Maury, N. Bahlawane, *Scientific Reports*, **6**, (2016) 37699.

9) L. A. Ladd, W. Paul, *Solid State Commun.* **7**, (1969) 425.

10) Z. Hiroi, H. Hayamizu, T. Yoshida, et al., *Chem. Mater,* **25,** (2013) 2202-2210.

11) Y. Muraoka, Z. Hiroi, *Appl. Phys. Lett.,* **80**, (2002) 583-585.

12) Z. Yang, C. Ko, S. Ramanathan, *J. Appl. Phys.*, **108**, (2010) 073708.

13) K. Shibuya, J. Tsutsumi, T. Hasegawa, et al., *Appl. Phys. Lett.*, **103**, (2013) 2.

14) H. Zhon, J. Li, Y. Xin et al., *Ceram. Int.*, **42**, (2016) 7655-7663.

15) G. Sun, H. Zhou, X. Cao et al., *Appl. Mater. Interfaces*, **8**, (2016) 7054-7059.

16) A. Kishimoto, Y. Kamakura, T. Teranishi et al., *Mater. Chem. Phys.*, **139**, (2013) 825-829.

17) D. Nagao, J. Fukushima, Y. Hayashi, H. Takizawa, *Ceram. Int.*, **41,** (2015) 14021-14028.

18) H. Takizawa, A. Hagiya, et al., *Chem. Lett.*, **37,** (2008) 714-715.

Manuscript received: September 29, 2017

Revised: November 27, 2017

Accepted: December 4, 2017